

# Genes located in a chromosomal inversion are correlated with territorial song in white-throated sparrows

W. M. Zinzow-Kramer<sup>†,\*</sup>, B. M. Horton<sup>†</sup>, C. D. McKee<sup>†</sup>, J. M. Michaud<sup>†</sup>, G. K. Tharp<sup>‡</sup>, J. W. Thomas<sup>§</sup>, E. M. Tuttle<sup>¶,\*\*</sup>, S. Yi<sup>††</sup> and D. L. Maney<sup>†</sup>

<sup>†</sup>Department of Psychology, <sup>‡</sup>Yerkes Nonhuman Primate Genomics Core, Emory University, Atlanta, GA, <sup>§</sup>NIH Intramural Sequencing Center, National Human Genome Research Institute, NIH, Rockville, MD, <sup>¶</sup>Department of Biology, <sup>\*\*</sup>The Center for Genomic Advocacy, Indiana State University, Terre Haute, IN, and <sup>††</sup>School of Biology, Georgia Institute of Technology, Atlanta, GA, USA

\*Corresponding author: W. M. Zinzow-Kramer, Department of Psychology, Emory University, Atlanta, GA 30322, USA. E-mail: wzinzow@emory.edu

The genome of the white-throated sparrow (*Zonotrichia albicollis*) contains an inversion polymorphism on chromosome 2 that is linked to predictable variation in a suite of phenotypic traits including plumage color, aggression and parental behavior. Differences in gene expression between the two color morphs, which represent the two common inversion genotypes (ZAL2/ZAL2 and ZAL2/ZAL2<sup>m</sup>), may therefore advance our understanding of the molecular underpinnings of these phenotypes. To identify genes that are differentially expressed between the two morphs and correlated with behavior, we quantified gene expression and territorial aggression, including song, in a population of free-living white-throated sparrows. We analyzed gene expression in two brain regions, the medial amygdala (MeA) and hypothalamus. Both regions are part of a 'social behavior network', which is rich in steroid hormone receptors and previously linked with territorial behavior. Using weighted gene co-expression network analyses, we identified modules of genes that were correlated with both morph and singing behavior. The majority of these genes were located within the inversion, showing the profound effect of the inversion on the expression of genes captured by the rearrangement. These modules were enriched with genes related to retinoic acid signaling and basic cellular functioning. In the MeA, the most prominent pathways were those related to steroid hormone receptor activity. Within these pathways, the only gene encoding such a receptor was *ESR1* (estrogen receptor 1), a gene previously shown to predict song rate in this species. The set of candidate genes we identified may mediate the effects of a chromosomal inversion on territorial behavior.

Keywords: Behavioral polymorphism, estrogen receptor alpha, RNA-seq, social behavior, WGCNA

Received 3 June 2015, revised 28 August 2015, accepted for publication 9 September 2015

The white-throated sparrow (*Zonotrichia albicollis*), a common North American songbird, provides a unique model to study the relationship between genes and behavior because it exhibits a chromosomal polymorphism linked to a behavioral polymorphism. In this species, the second chromosome occurs in two arrangements, ZAL2 and ZAL2<sup>m</sup> (Thornycroft 1975). These arrangements differ at a minimum by a pair of pericentric inversions that span ~98 Mb, representing about 10% of the genome (Thomas *et al.* 2008). Inversions can lead to changes in genetic sequences that can have profound effects on phenotype. Although inversion polymorphisms have been described in multiple species, from *Drosophila* to humans (Kidd *et al.* 2008; Ma & Amos 2012; White 1977), the consequences of such rearrangements are not completely understood. The white-throated sparrow provides a vertebrate model of an inversion polymorphism that clearly affects the brain and behavior.

Within a population, approximately half of the individuals of both sexes are heterozygous for the chromosomal arrangement (ZAL2/ZAL2<sup>m</sup>) (Thornycroft 1975). These individuals have contrasting white and black stripes on the crown and are members of the 'white-striped' (WS) morph (Lowther 1961). The other half of the population is homozygous for the ZAL2 arrangement (ZAL2/ZAL2), a genotype that results in a 'tan-striped' (TS) phenotype characterized by tan and brown stripes on the crown (Lowther 1961). Birds homozygous for ZAL2<sup>m</sup> are extremely rare, occurring at a frequency of roughly 1 in 500 (Horton *et al.* 2013). Their scarcity is due at least in part to a disassortative mating system; within a population, nearly all breeding pairs consist of one TS and one WS bird (Lowther 1961). WS male–WS female pairings, which are necessary to create a ZAL2<sup>m</sup>/ZAL2<sup>m</sup> homozygote, make up <2.5% of breeding pairs (Falls & Kopachena 2010). This mating system maintains the ZAL2<sup>m</sup> arrangement in the population and keeps the frequency of ZAL2<sup>m</sup>/ZAL2<sup>m</sup> homozygotes very low. Because of its near-constant state of heterozygosity, recombination within the ZAL2<sup>m</sup> inversions is profoundly suppressed (Davis *et al.* 2011; Huynh *et al.* 2011). Limited gene flow between the ZAL2 and ZAL2<sup>m</sup> haplotypes has caused the accumulation of single nucleotide and insertion/deletion polymorphisms and thus genetic differentiation

of the rearranged region. Davis *et al.* (2011) estimated that there are on the order of 1870 nonsynonymous differences between the ZAL2 and ZAL2<sup>m</sup> alleles inside the inversions, affecting approximately 1100 genes. This genetic differentiation between the two chromosomes must be responsible for the phenotypic differences observed between the two plumage morphs.

The chromosomal rearrangement is of particular interest because it affects social behaviors (Maney 2008; Tuttle 2003). Individuals with the ZAL2<sup>m</sup> chromosome engage in more aggression and less parental care than individuals without it (Falls & Kopachena 2010). For example, WS birds of both sexes sing more and are thus more vocally aggressive than their TS counterparts (Horton *et al.* 2014b; Kopachena & Falls 1993a; Lowther 1962). On the other hand, TS birds provision nestlings more frequently than WS birds; this effect is especially pronounced in males (Horton & Holberton 2010; Horton *et al.* 2014b; Knapton & Falls 1983; Kopachena & Falls 1993b). WS males seek out more extra-pair copulations than TS males, who instead guard their mates more closely (Formica & Tuttle 2009; Tuttle 2003). The two phenotypes represent alternative reproductive strategies (Trivers 1972), in which individuals maximize investment in competition and mate finding or investment in mate guarding and parenting (Tuttle 2003). Because the strategy depends on the presence or absence of the ZAL2<sup>m</sup> chromosomal arrangement, this polymorphism represents a powerful genetic target with which to understand the molecular mechanisms underlying the associated behaviors.

In this study, we employed a genome-wide approach to identify genes associated with behavior and the chromosomal rearrangement. First, we measured natural variation in aggressive responses to simulated territorial intrusions (STIs) in a free-living population of male white-throated sparrows early in the breeding season. We then generated and analyzed transcriptomes from two brain regions thought to be important for social behavior, namely the medial amygdala (MeA, formerly called nucleus taeniae in birds; for a review of its homology, see O'Connell & Hofmann 2011) and the hypothalamus (HYP). We chose these regions because they are part of a well-known social behavior network that responds during social encounters (Goodson *et al.* 2005; Maney *et al.* 2008). In the MeA and HYP in particular, the expression of genes that confer sensitivity to sex steroids, such as estrogen receptor alpha (ER $\alpha$ ), was already known to be correlated with territorial responses (Rosvall *et al.* 2012) and to differ between the morphs (Horton *et al.* 2014a). Our goal in this study was to expand our understanding of the genetic basis of this behavioral polymorphism beyond a handful of genes. Because the neurochemical and neuroanatomical pathways that regulate social behaviors such as aggression rely on the expression of many genes (reviewed in Anholt & Mackay 2012; Nelson & Chiavegatto 2001), we employed a network-based approach to identify groups of co-regulated genes (modules) with expression that is correlated with plumage morph, song rate or physical aggression. Toward this goal, we used weighted gene co-expression network analysis (WGCNA) (Zhang & Horvath 2005), which has previously been used to relate gene expression to physiological and behavioral traits (Drnevich *et al.* 2012; FiltEAU

*et al.* 2013; Fuller *et al.* 2007; Ghazalpour *et al.* 2006; Hilliard *et al.* 2012; Langfelder & Horvath 2008). We then examined the gene modules to identify candidate genes and molecular pathways linked to aggressive behavior. By taking this whole transcriptome approach, we aimed to better understand the molecular mechanisms underlying territorial aggression and, more generally, the effects of inversion polymorphisms on gene expression.

## Materials and methods

### Ethical note

All studies were performed with the approval of the Emory University Institutional Animal Care and Use Committee, with appropriate state (Maine Inland Fisheries and Wildlife and Federal U.S. Geological Survey and U.S. Fish and Wildlife Service) permits, and with permission from the Forest Society of Maine.

### Behavioral assay and data collection

Our study population consisted of free-living white-throated sparrows in the Hemlock Stream Forest, Argyle, Maine. To correlate behavior with gene expression, we performed behavioral tests prior to tissue collection. We quantified territorial aggression during the peak of territorial behavior (7 May–3 June), after pair formation and territory establishment but prior to or early in the stage of incubation (Falls & Kopachena 2010). Prior to behavioral observations, birds were captured in mist nets using conspecific song playback and banded with color bands and aluminum USGS identification bands. At the time of capture, morph was determined based on plumage color (Watt 1986), and sex was determined by the presence or absence of a cloacal protuberance or brood patch. Morph was later confirmed by polymerase chain reaction genotyping of the *DSE* locus (Horton *et al.* 2013; Thomas *et al.* 2008), and sex was confirmed by gonads during tissue collection (see below).

Simulated territorial intrusions were performed as described by Horton *et al.* (2014b). Briefly, at least 3 days after they were banded, each resident male was exposed to a caged, live male decoy placed onto his territory while conspecific song was played via an adjacent speaker. We used four different male decoys, two of each morph, and four song exemplars chosen from those used in the previous study. In this species, behavioral responses to STI can depend on the morph of the intruder (Horton *et al.* 2012; Kopachena & Falls 1993a). To control for this potential variation, we performed two STIs on each male, on consecutive days but at the same time of day (0630–1230 h Eastern Daylight Time, EDT), presenting either a TS or WS decoy. The morph of the intruder was counterbalanced such that half of the pairs were presented with a TS decoy first, and the other half were presented with a WS decoy first. For all analyses, data on behavioral responses were averaged across the two STIs for each individual. Behavioral data were collected from 9 TS males and 10 WS males.

Each STI was monitored by two observers and behaviors were recorded as previously described (Horton *et al.* 2014b). After the male was detected within 30 m of the decoy, playback continued for 10 min. We recorded behaviors indicative of territorial aggression in *Zonotrichia* species. The physical behaviors measured were latency to approach (the time from start of playback until the resident male arrived), number of directed flights over the decoy, time spent within 5 m and within 2 m of the decoy and distance of closest approach to the decoy (Kopachena & Falls 1993a; Wingfield & Hahn 1994). We recorded three types of vocalizations that commonly occur during agonistic encounters and that signal aggression (chip calls, trills and songs) (Collins & Houtman 1999; Falls & Kopachena 2010).

### Statistical analysis of behavioral data

Because the behavioral data were not normally distributed (based on Shapiro–Wilk tests), we tested for morph differences in behavior using the Wilcoxon rank sum test. To reduce the number of comparisons, we used principal component analysis (PCA) to

construct a composite physical aggression score (first principal component, PC1) from three physical behaviors (Horton *et al.* 2012). The behaviors used in the PCA were time within 2 m, closest approach and flights. We chose to exclude time in 5 m because variation in this measure within the sample population was low. Physical latency scores were not recorded for trials in which the resident male was within the area at the start of playback. Because PCA does not tolerate missing data, we did not include latency in the PCA. The data on closest approach were square root transformed to achieve normality prior to PCA calculations. Statistical tests and PCA were carried out using JMP v. 10.0 (SAS, Cary, NC, USA).

### Tissue collection and RNA extraction

Because we were interested in identifying the genes and networks related to the propensity and capacity to respond to challenge rather than those induced by the act of responding and the challenge itself, we collected birds on the day following the second STI. A total of 19 males (10 WS and 9 TS) were collected the day after the second STI using mist nets and song playback. Playbacks were started between 0700 and 1400 h EDT, which was  $5.35 \pm 2.03$  h after sunrise, and were balanced so that birds of both morphs were collected at earlier and later time points. Average latency to capture was  $2.79 \pm 0.14$  min after the onset of the song playback, with a maximum of 4.0 min. Immediately after capture, birds were sacrificed by isoflurane overdose and brains were rapidly dissected, frozen on dry ice and stored at  $-80^{\circ}\text{C}$ . At the end of the field portion of the study, tissues were shipped to Atlanta on dry ice and stored at  $-80^{\circ}\text{C}$  until sectioning. Brains were cryosectioned in the coronal plane at  $300\text{ }\mu\text{m}$  thickness and the regions of interest were microdissected from frozen sections using a 1.0-mm diameter punch tool (Fine Science Tools, Foster City, CA, USA). The ventromedial telencephalon, which contained the MeA, was sampled in each hemisphere in two consecutive sections for a total of four punches, which were pooled for RNA extraction (Fig. S1a). For most of these punches, MeA constituted the majority of the sampled tissue. For the HYP, all punches were centered on the midline such that they contained tissue from both hemispheres. One punch was made immediately ventral to the anterior commissure and included the caudal portion of the medial preoptic area (POM), the paraventricular nucleus (PVN) and the anterior hypothalamus (Fig. S1b). A second punch was made ventral to the first and included the ventromedial hypothalamus (VMH). Both HYP punches were made in two consecutive  $300\text{ }\mu\text{m}$  sections for a total of four punches, which were pooled for RNA extraction. RNA was extracted using the Qiagen Allprep DNA/RNA micro kit (Qiagen, Valencia, CA, USA) with modification, as follows. Punches were homogenized in RLT plus  $\beta$ -mercaptoethanol using a pellet mixer. An equal volume of phenol:chloroform:isoamyl alcohol (25:24:1) at pH 7.5 was added to each sample. Samples were further homogenized by passing them through a QiaShredder column (Qiagen). Phases were separated by spinning for 15 min at  $4^{\circ}\text{C}$ , and the aqueous phase was collected and further processed according to the manufacturer's protocol.

### RNA sequencing library preparation

Library preparation and sequencing were performed at the Emory Yerkes Nonhuman Primate Genomics Core. The quality of total RNA was assessed on an Agilent bioanalyzer instrument (Agilent Technologies, Santa Clara, CA, USA). RNAseq libraries were constructed using the Illumina TruSeq RNA Sample Preparation Kit v2 (Illumina Inc., San Diego, CA, USA) according to the manufacturer's protocol. Briefly, polyadenylated transcripts were purified on oligo-dT magnetic beads, chemically fragmented, reverse transcribed using random hexamers and incorporated into barcoded cDNA libraries. Libraries were validated by microelectrophoresis, quantified, pooled and clustered on an Illumina TruSeq v3 flowcell. The clustered flowcell was sequenced on an Illumina HiSeq 1000 in 100 base paired end-read reactions. We obtained 11–22 million reads per sample.

### Creation of an enhanced reference genome

The reference genome, downloaded from NCBI (*Z. albicollis* 1.0.1, GCA\_000385455.1, Tuttle *et al.* in review), was generated from a

bird homozygous for the ZAL2 haplotype. To eliminate potential mapping bias against reads that originated from the ZAL2<sup>m</sup> chromosome, we created an enhanced reference genome that contained sequences representing both ZAL2 and ZAL2<sup>m</sup> haplotypes within the inversion. To create this enhanced version of the white-throated sparrow genome, we first performed a  $\sim 30\times$  whole-genome shotgun sequencing of a 'superwhite' bird homozygous for the ZAL2<sup>m</sup> chromosome (Horton *et al.* 2013; SRA accession pending). NOVOALIGN (novocraft.com, version 3.00.05) was used to map the reads to the reference genome using '-r RANDOM -l PE 510,150-0 SAM' option. To identify single nucleotide polymorphisms (SNPs) between the ZAL2 and ZAL2<sup>m</sup> chromosomes, SAMTOOLS v1.1 (Li *et al.* 2009) was used to call SNPs between the reference genome and the superwhite genome. High-quality (genotype quality score = 99) homozygous non-reference SNPs were then used to generate alternative contigs representing ZAL2<sup>m</sup> sequences within the inversion (File S1). To create these ZAL2<sup>m</sup> contigs, we first identified NCBI genome contigs that mapped to ZAL2 via orthology with zebra finch (*Taeniopygia guttata*) chromosome 2 (Davis *et al.* 2011; Romanov *et al.* 2011) based on sequence similarity and gene annotations. We then created ZAL2<sup>m</sup> versions of the contigs that mapped within the inversion using the Genome Analysis Toolkit v3.2.2 tool FASTAALTERNATIVEREFERENCEMAKER (McKenna, *et al.* 2010). We also generated assemblies of rRNA and the mitochondrial genome derived from these whole-genome shotgun sequences (Files S2–S3). Our final enhanced reference genome was composed of the NCBI reference genome (*Z. albicollis* 1.0.1) plus ZAL2<sup>m</sup> versions of contigs located within the inversion, rRNA, and a mitochondrial genome.

### RNA-seq mapping and gene annotation

RNA-seq reads were mapped to the enhanced version of the white-throated sparrow reference genome described above. We used the STAR\_2.3.0e aligner (Dobin *et al.* 2013) to map the reads to the modified reference allowing each read to map to at most two loci (outFilterMultimapNmax = 2). Reads that did map within the inversion to both the reference and alternative contigs were then filtered to retain just the primary mapping location. All other dual mappings were excluded. Retained mappings to the alternate contigs were relabeled to conform to the unmodified reference contig names. Reads were assigned to genes using the HTSeq v0.6.1 function htseq-count (Anders *et al.* 2015) based on NCBI RefSeq annotations.

### Network analysis

To identify groups of co-expressed genes (modules) correlated with both song rate and morph, we performed WGCNA (Zhang & Horvath 2005) for the MeA and HYP samples separately. Network analyses were performed using R version 3.1.1 (<http://www.r-project.org>) and functions in the WGCNA library version 1.41.1 (Langfelder & Horvath 2008). Genes with unreliable expression (defined as 0 reads in more than half of the samples) were removed from the dataset. This filtering did not selectively remove genes expressed only in one morph. Of the 3191 genes removed, 3185 of the genes had 0 reads in at least three TS and three WS samples and all of the genes removed had 0 reads in at least one TS and one WS sample. After this screen, 13 426 and 13 605 genes remained in the MeA and HYP datasets, respectively. Prior to network analysis, read counts were transformed using the varianceStabilizingTransformation function in the DESeq2 v1.4.5 package for R (Love *et al.* 2014). We performed WGCNA in R using functions in the WGCNA library (Langfelder & Horvath 2008). To create the weighted gene co-expression network, a weighted adjacency matrix was created for all pairwise gene comparisons across samples based on the absolute value of the Pearson correlation raised to the power  $\beta$ . The power  $\beta$  was determined empirically by examining the scale-free fit across a range of powers. The adjacency matrix was transformed into a topological overlap (TO) Matrix. A dendrogram was constructed using average linkage hierarchical clustering based on the distance measure calculated as 1-TO. Next, modules were identified by cutting the dendrogram using the WGCNA function DYNAMICTREECUT (Langfelder *et al.* 2008). Finally, modules with similar expression patterns were merged. The algorithm labels each module with an arbitrarily assigned color; the

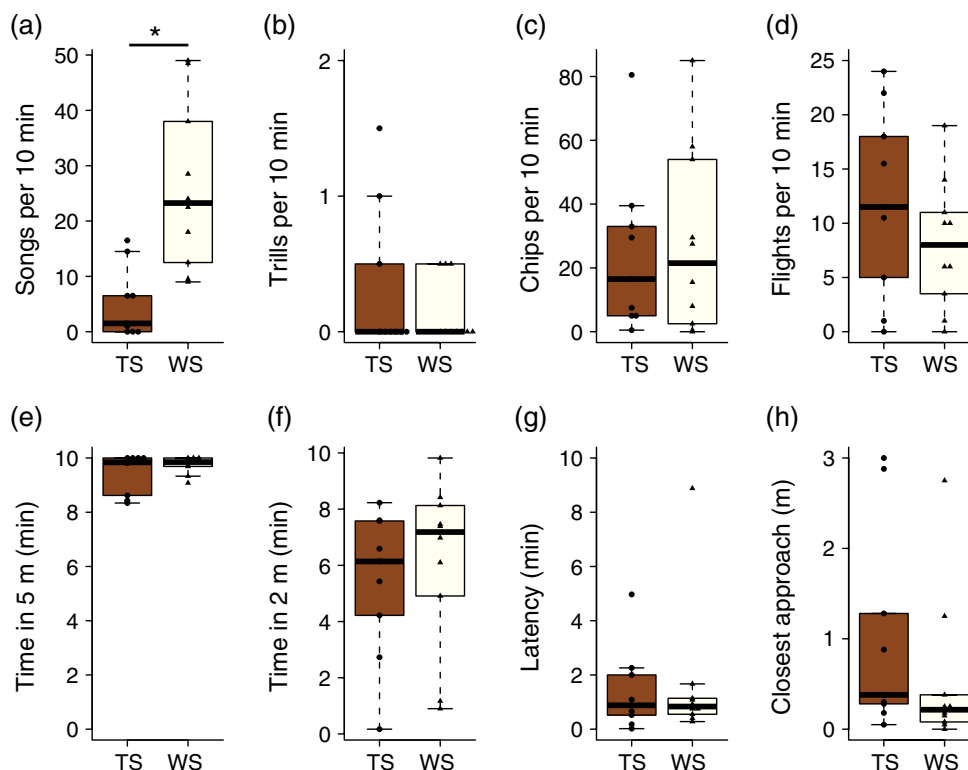


**Figure 1: Behavioral responses to STIs.** Vocal measures of aggression were average (a) number of songs, (b) number of trills and (c) number of chips recorded per 10-min STI. Measures of physical aggression were average (d) number of flights per 10-min STI, (e) time spent within 5 m, (f) time spent within 2 m, (g) latency and (h) distance of closest approach. Scores for individual birds are represented by circles (TS) or triangles (WS). Whiskers represent 1.5 times the inner quartile range. \* $P < 0.005$

gray module is reserved for genes not assigned to a proper module. The WGCNA function `blockwiseModules` was used to create the network and identify modules in one step. The function offers many choices of parameters for each step in the process. Using the scale-free topology criterion as described in Zhang & Horvath (2005), the power  $\beta$  was set to 4 and 7 for the MeA and HYP networks, respectively. Additional values used to create both the MeA and HYP networks were: `TOMType=unsigned`, `deepSplit=2`, `minModuleSize=30`, `reassignThreshold=0`, `mergeCutHeight=0.25` and `pamRespectsDendro=FALSE`. All other parameters were left at default values.

### Statistical analysis of gene co-expression networks

The WGCNA program was used to calculate the module membership (MM) for each gene, which is the correlation between a gene's expression profile and the module eigengene (ME, the PC1 of module gene expression). To identify modules composed of genes that were highly correlated with the trait of interest, we calculated Pearson correlation coefficients between MEs and traits of interest (morph, song rate and PC1 for physical aggression). We chose song rate (number of songs during the 10-min STI) as a measure of vocal aggression because song is the primary vocalization used to deter territorial intruders (Falls 1988) and the rate at which it is used in territorial defense differs dramatically between morphs in our study population (Horton *et al.* 2014b and Fig. 1). We also calculated gene significance (GS) as the Pearson correlation coefficient between the expression of each gene and each trait or *EGR1* expression. For correlation analyses, data on song rate were square root transformed to achieve normality. Pearson correlations were computed using the WGCNA `cor` function. VISANT 4.3.2 (Hu *et al.* 2004) was used to

visualize the networks represented by the top modules. Intramodular connectivity ( $k_{IN}$ ), used to identify well-connected genes, was calculated for each gene as the sum of its network connections with other module members. To compare MeA and HYP networks, the function `modulePreservation` was used. This function computes preservation statistics for a test network (HYP) compared with a reference network (MeA). This function also computes gene membership overlap and Fisher's exact test  $P$ -values between modules in each network.

### Identification of genes on chromosome 2

We chose to use the annotation of the chicken (*Gallus gallus*) genome to assign genes to *Z. albicollis* chromosome 2 (ZAL2/2<sup>m</sup>) because the chicken genome was better annotated than the zebra finch genome in the Ensembl database. Chicken gene names and chromosome annotations were downloaded from Biomart ([www.ensembl.org/biomart](http://www.ensembl.org/biomart), Ensembl Genes 75). We assigned 891 genes to ZAL2/2<sup>m</sup> based on homology to genes on chicken chromosome 3, which is orthologous to ZAL2/2<sup>m</sup> (Thomas *et al.* 2008). Because this analysis is based on synteny with chicken chromosome 3, any loss of synteny between the species would result in misidentifying ZAL2/2<sup>m</sup> genes. To capture ZAL2/2<sup>m</sup> genes not represented in the chicken genome, we identified a list of 32 white-throated sparrow contigs that map to ZAL2/2<sup>m</sup> (see above). A total of 1183 genes mapped to one of these contigs. It is possible that some smaller contigs representing ZAL2/2<sup>m</sup> sequences were missing from our list, which would have resulted in missing any ZAL2/2<sup>m</sup> genes located on those contigs. There was good correspondence between these two methods; 877 genes mapped to ZAL2/2<sup>m</sup> using both methods. After summing the genes that mapped using at least one method, a total of 1197 genes were assigned to ZAL2/2<sup>m</sup>.



### Gene function and pathway analysis

#### Gene ontology

Gene names were converted to the corresponding zebra finch Ensembl IDs for gene ontology (GO) enrichment analysis using the CORNA v1.3 package in R (Wu & Watson 2009). Gene conversions were performed using ID conversion tables downloaded from Ensembl (Flicek *et al.* 2014). Fisher's exact test was performed using the list of genes in the network as the background. We considered terms with  $P < 0.05$  to be significantly over-enriched in the module. To prioritize enriched terms most likely to be relevant to module function, terms annotated with fewer than three genes or represented by only one gene in the module were removed from the list. To identify genes annotated with a specific term, gene names were uploaded to the Database for Annotation, Visualization and Integrated Discovery (DAVID 6.7; Huang *et al.* 2009). We searched the functional annotation table for genes annotated with the term (e.g. 'transcription factor activity'). Because zebra finch genes were poorly annotated in the DAVID database, human gene annotations were used.

#### Pathway analysis

Lists of gene name annotations for each module were used for ingenuity pathway analysis (IPA) using the core analysis procedure and the human genome as background. IPA calculates canonical pathway enrichment using a right-tailed Fisher's exact test. A  $-\log(P\text{-value}) > 1.3$  was considered significant.

## Results

### Behavior

Of the behaviors recorded, only song rate differed between the morphs, which is consistent with previous results from this population (Horton *et al.* 2014b). In our sample population, TS males sang less than WS males in response to STI (Fig. 1, Wilcoxon  $W = 6$ ,  $P < 0.005$ ). There was no difference between the morphs in any of the other responses to the STIs (trills, chips, flights over decoy, time spent within 5 m, time spent within 2 m, latency to respond and closest approach; see Fig. 1). Statistical power was 0.95 for songs, 0.06 for chips, 0.05 for latency and 0.14–0.19 for the other behaviors. Although our power to detect morph differences in behaviors other than singing was low in this study, we replicated our results from a larger study (Horton *et al.* 2014b). The PC1 for physical aggression explained 73% of the variation, and did not significantly differ between the morphs (Wilcoxon  $W = 58$ ,  $P = 0.29$ ).

### Gene networks in the MeA

The WGCNA identified 17 modules in the MeA samples. To relate module expression to trait expression, we calculated the correlation between the ME of each module and the three traits of interest (morph, song rate and PC1 physical aggression) (Fig. 2a). Correlations for only one module, greenyellow, had  $P$ -values  $< 0.01$ . After Bonferroni correction (significance threshold  $\alpha = 9.8\text{e-}4$ ), the greenyellow module remained significantly correlated with both morph ( $r = 0.99$ ,  $P = 9\text{e-}18$ ) and song rate ( $r = 0.74$ ,  $P = 3\text{e-}4$ ). In contrast, no modules were correlated with the PC1 for physical aggression (Fig. 2a and Table S1) or any of the individual behaviors used in the PCA (data not shown). Next, to relate expression variability in individual genes to trait variability, we calculated GS measures for each gene (Langfelder & Horvath 2008). As expected, the

greenyellow module, which was correlated with both morph and song rate, contained genes that were also highly correlated with both traits (Fig. 2c and Table S2). The majority of the genes in the greenyellow module (115 of 157) were located within the inversion on ZAL2/2<sup>m</sup> (Figs. 2c, 3a and Table S2).

### Gene networks in the HYP

The WGCNA identified 83 modules in the HYP dataset. Only one module, black, had module-trait correlations with  $P$ -values  $< 0.01$ . After Bonferroni correction (significance threshold  $\alpha = 2\text{e-}4$ ), the ME of the black module remained significantly correlated with both morph ( $r = -0.99$ ,  $P = 6\text{e-}16$ ) and song rate ( $r = -0.75$ ,  $P = 2\text{e-}4$ ). As with the MeA modules, no ME was significantly correlated with PC1 physical aggression (Fig. 2b and Table S3) or any of the individual physical behaviors used in the PCA (data not shown). The black module was composed of 511 genes that were highly correlated with both song and morph, and 226 of these genes were located within the inversion on ZAL2/2<sup>m</sup> (Figs. 2d, 3b and Table S4).

### The modules correlated with song and morph share chromosome 2 genes

A large percentage of both the MeA greenyellow and the HYP black module was composed of differentially expressed genes located on chromosome 2 (Fig. 3). To assess the similarity between these two modules, we used the WGCNA function modulePreservation to compute preservation statistics and a cross-tabulation table between the MeA and HYP modules. Preservation statistics were summed into one variable, the  $Z_{\text{summary}}$ ; a  $Z_{\text{summary}}$  score  $> 10$  was considered strong evidence for module preservation (Langfelder *et al.* 2011). The  $Z_{\text{summary}}$  for the MeA greenyellow module in the HYP network was  $> 40$ . There was also significant overlap in gene membership between the MeA greenyellow and HYP black modules (Fig. S2). We found 85 genes located within both modules, which was significantly more than would be expected by chance (Fisher's exact test,  $P < 5.0\text{e-}80$ ) and 70 of these shared genes were located on ZAL2/2<sup>m</sup>.

### Biological pathways in the modules correlated with morph and song rate

We utilized two strategies to identify genes that may play key roles in the behavioral polymorphism in this species and thus territorial behavior generally. First, we looked for overrepresentation of genes belonging to known biological pathways. We used both pathway (IPA tool) and GO enrichment analyses to identify pathways represented by the genes in the modules that were significantly correlated with song. There was a strong correlation between MM and GS song rate ( $r = 0.65$ ,  $P < 3\text{e-}20$  MeA greenyellow;  $r = 0.65$ ,  $P < 1\text{e-}62$  HYP black), which suggests a relationship between connectivity within the module and behavioral relevance. In order to identify the most behaviorally relevant pathways, we filtered the results for pathways that contained gene(s) with high MM (top 50)

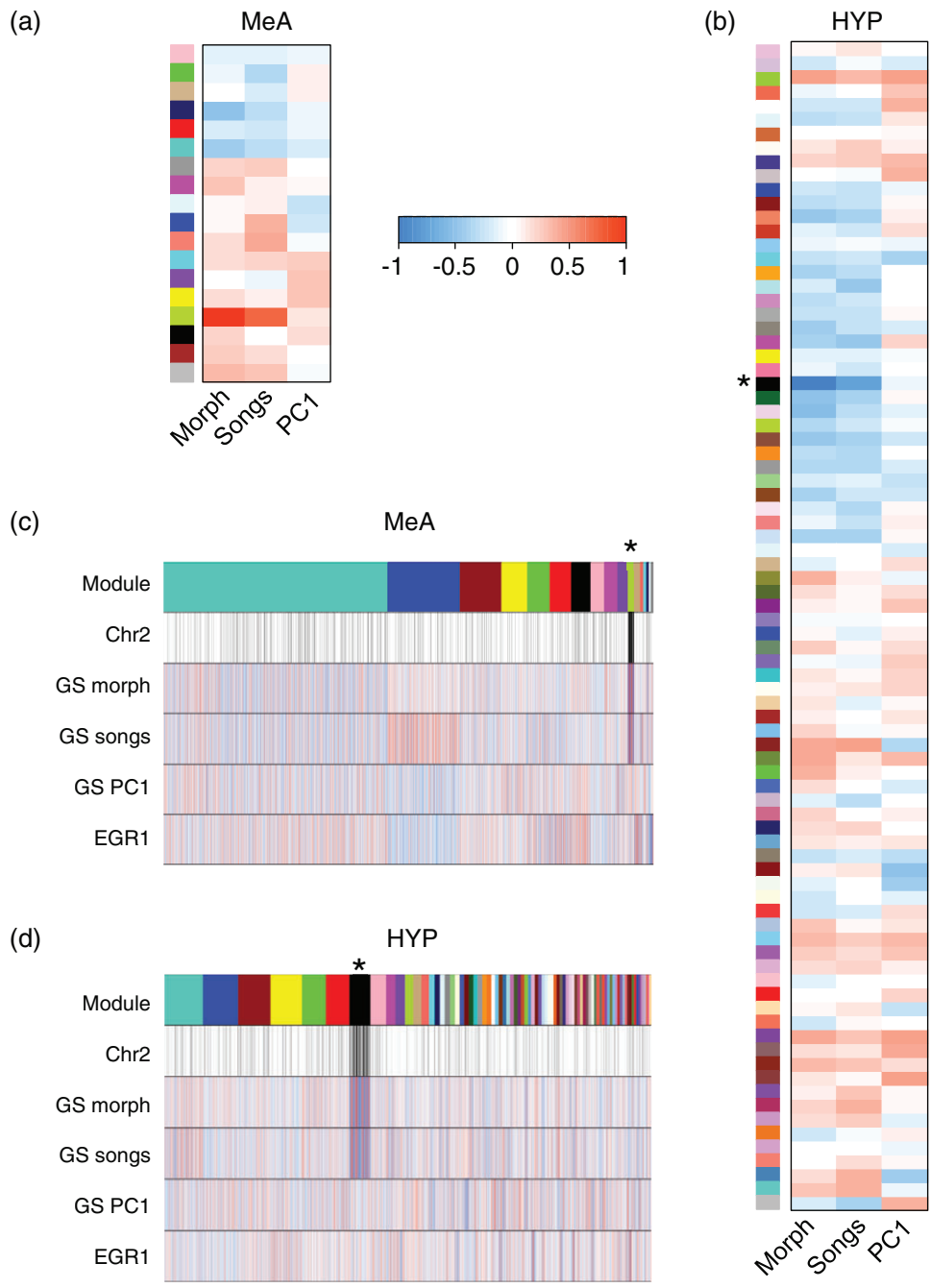


**Figure 2: Correlations between gene expression and traits.** Correlations were calculated between MEs and morph, song rate or PC1 for physical aggression. In the MeA (a) and the HYP (b), each row corresponds to a module and columns correspond to each trait. The color of each cell indicates the value of the correlation coefficient. Positive correlations are red, and negative correlations are blue, as indicated by the color scale bar. In the MeA (c) and the HYP (d), genes are ordered according to membership within the modules. The color bar in the top row indicates the module to which each gene is assigned; genes assigned to the gray module are not shown. In the second row, genes located on ZAL2/2<sup>m</sup> are indicated by black bars. Rows 3–5 represent the correlation between the expression of each individual gene and the trait indicated (GS). Row 6 represents the correlation between the expression of each gene and EGR1 expression. Each gene is represented by a line, and the color of the line indicates the correlation coefficient, as indicated by the color scale bar. Correlation and *P*-values are provided in Tables S1 and S3. \*Modules correlated with both morph and song.

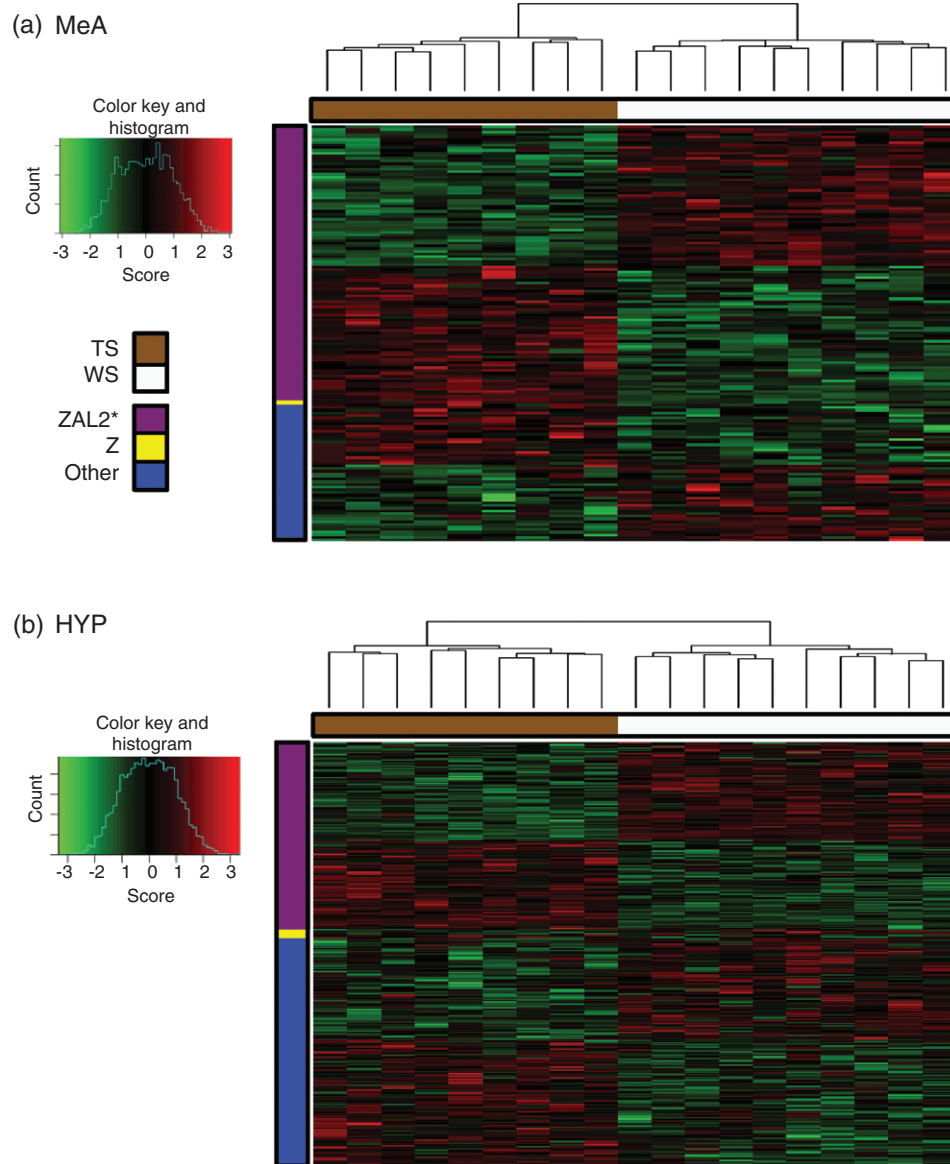


**Figure 3: Heat map of expression for individual genes in the modules correlated with song and morph.** (a) MeA greenyellow module, (b) HYP black module. Columns represent samples, sorted by hierarchical clustering. Morph is indicated by the color bar at the top (tan = TS and white = WS birds). Rows represent genes, sorted by chromosome location and then by hierarchical clustering. The color bar on the left indicates the chromosome location of the genes. Genes were assigned to chromosome 2 (ZAL2, purple), chromosome Z (Z, yellow) or other (all genes not assigned to ZAL2 or Z, blue). Expression (score) is represented by the standardized residual [score = (value-mean)/SD]. Red, increases; green, decreases; black, no change relative to the mean. \*All ZAL2 genes located within these two modules were also located within the inversion.

In the MeA greenyellow module, IPA identified 22 pathways that were significantly overrepresented; 17 of these pathways contained highly connected genes (Table 1). Most of these pathways shared the signaling molecules MAP3K7, TGFB2, NFKB1E or SOS1. In the HYP black module, IPA identified 42 pathways that were significantly overrepresented; 24 of these pathways contained highly connected genes (Table 2).

The GO analysis identified 18 enriched terms that were represented by two or more genes in the MeA greenyellow module. Enriched GO terms involved microtubule activity (GO: 0034453, GO: 0003777 and GO: 0007018), fatty acid metabolic processes (GO: 0000038 and GO: 0006635), mitochondria (GO: 0005739), ADP binding (GO: 0043531), kinase activity (GO: 0000186 and GO: 0006469) and locomotory behavior (GO: 0007626) (Table S5). We

**Table 1:** Pathways significantly overrepresented in the MeA greenyellow module\*

Ingenuity canonical pathways	$-\log(P\text{-value})$	Ratio	Genes
Glucocorticoid receptor signaling	3.07	0.027	MAP3K7, TGFB2, NFKBIE, GTF2H5, SOS1, ESR1, TAF5L
PPAR $\alpha$ /RXR $\alpha$ activation	2.40	0.028	MAP3K7, ACOX1, TGFB2, NFKBIE, SOS1
ER signaling	2.19	0.031	GTF2H5, SOS1, ESR1, TAF5L
Regulation of IL-2 expression in activated and anergic T lymphocytes	1.96	0.038	TGFB2, NFKBIE, SOS1
Hepatic cholestasis	1.83	0.025	MAP3K7, TGFB2, NFKBIE, ESR1
Thyroid hormone biosynthesis	1.76	0.333	IYD
PPAR signaling	1.76	0.032	MAP3K7, NFKBIE, SOS1
IL-17A signaling in fibroblasts	1.75	0.057	MAP3K7, NFKBIE
tRNA charging	1.66	0.051	AARS2, IARS2
Role of PKR in interferon induction and antiviral response	1.64	0.050	MAP3K7, NFKBIE
Geranylgeranyldiphosphate biosynthesis	1.64	0.250	GGPS1
<i>Trans</i> , <i>trans</i> -farnesyl diphosphate biosynthesis	1.54	0.200	GGPS1
IL-6 signaling	1.52	0.026	MAP3K7, NFKBIE, SOS1
PKC $\theta$ signaling in T lymphocytes	1.50	0.025	MAP3K7, NFKBIE, SOS1
Assembly of RNA polymerase II complex	1.46	0.040	GTF2H5, TAF5L
PI3K/AKT signaling	1.45	0.024	ITGA2, NFKBIE, SOS1
CD27 signaling in lymphocytes	1.43	0.039	MAP3K7, NFKBIE

\*IPA identified 24 pathways significantly enriched in the MeA greenyellow module. Only those pathways that also contain well-connected genes are shown. Ratio: Number of pathway genes in the greenyellow module divided by the total number of genes in the pathway.

identified 74 enriched terms that were represented by two or more genes in the HYP black module. To focus on the terms most relevant for the HYP black module, we looked for terms that contained hub genes. These terms involved activation of mitogen-activated protein kinase (MAPK) activity (GO: 0004709 and GO: 0000186), prenyltransferase activity (GO: 0004659), isoprenoid biosynthetic processes (GO: 0008299) and extracellular matrix organization (GO: 0030198) (Table S5).

#### Identification of biologically relevant hub genes

In the second approach to identify biologically relevant genes, we used GO annotations to identify transcriptional regulators within the module. Because well-connected transcription factors may coordinate the expression of multiple genes, we searched for well-connected (aka 'hub') genes within the module (Fig. 4 and Table S2 and S4) that were annotated with the GO term transcription factor activity. In the MeA greenyellow module, we identified three genes with this GO annotation: *ESR1*, *TAF5L* and *GTF2H5*. All three of these genes were also represented in the IPA pathways identified for that module. The most well-connected gene within the module, *EPM2A*, while not a transcription factor, was strongly connected to both *TAF5L* and *ESR1* (see Fig. 4a). Other well-connected genes that have a role in transcription were *C1D*, *OLIG3* and *STON1*. In the HYP black module, hub genes annotated with transcription factor activity were *TAF5L*, *ACSS1*, *AGT* and *MYF5*. Among these genes, only *TAF5L* was strongly connected to the other hub genes (Fig. 4b). Our ability to speculate about the functional roles and importance of hub genes was limited for both modules

by the information available about each gene. Well-connected genes not discussed here, particularly ones that are not annotated (e.g. LOC designations) may also play interesting roles.

#### Discussion

In this study, our aim was to identify genes that correlate with behavior, and thus are candidates for mediating the effects of a chromosomal inversion on social behavior in this species. In order to accomplish this aim, we quantified territorial behavior in free-living males and subsequently analyzed gene expression in brain regions that are part of a social behavior network (Goodson 2005) and previously linked with territorial responses in this species (Horton *et al.* 2014a). Using gene co-expression network analysis, we found one module significantly correlated with both morph and song rate in each of these regions. In contrast, no modules were correlated with physical aggression, a behavior that did vary among individuals but did not differ between the morphs (see also Horton *et al.* 2014b).

The positive correlation between MM and GS for song in both the MeA greenyellow and HYP black modules indicates that genes central to the network (i.e. hub genes) are also highly correlated with song rate. Because of their centrality within the module, hub genes have the potential to be key drivers of the gene co-expression network. Some of the most well-connected hub genes in these two modules are involved in basic cellular processes likely common to most cell types. For example, the gene *EMP2A*, which is a hub in both the greenyellow MeA and black HYP modules (Fig. 4), encodes the protein laforin, which maintains the phosphorylation state



**Table 2:** Pathways significantly overrepresented in the HYP black module\*

Ingenuity canonical pathways	$-\log(P\text{-value})$	Ratio	Genes
RAR activation	2.77	0.057	PRKCD, PNRC1, AKT3, MAP3K5, NT5C1B, SMAD6, TGFB2, PRKCI, GTF2H5, ERCC3
RANK signaling in osteoclasts	2.23	0.068	MAP3K7, AKT3, MAP3K5, NFKBIE, MAP3K4, NFATC1
Gαq Signaling	2.21	0.054	PRKCD, AKT3, PLCB4, HTR2C, PRKCI, NFKBIE, NFATC1, FNBP1
Type II diabetes mellitus signaling	2.21	0.060	MAP3K7, PRKCD, AKT3, MAP3K5, SOCS5, PRKCI, NFKBIE
Superpathway of D-myo-inositol (1,4,5)-trisphosphate metabolism	2.02	0.125	IMPA2, ITPKA, BPNT1
LPS-stimulated MAPK signaling	1.94	0.069	MAP3K7, PRKCD, MAP3K5, PRKCI, NFKBIE
HGF signaling	1.87	0.057	MAP3K7, PRKCD, AKT3, MAP3K5, PRKCI, MAP3K4
VDR/RXR activation	1.83	0.064	SERPINB1, PRKCD, TGFB2, PRKCI, HES1
CD27 signaling in lymphocytes	1.81	0.077	MAP3K7, MAP3K5, NFKBIE, MAP3K4
Methylthiopropionate biosynthesis	1.73	1	ADI1
Production of nitric oxide and reactive oxygen species in macrophages	1.72	0.044	MAP3K7, PRKCD, AKT3, MAP3K5, PRKCI, NFKBIE, MAP3K4, FNBP1
G-protein coupled receptor signaling	1.67	0.039	AKT3, MC3R, PLCB4, CNR1, HTR1E, HTR2C, FSHR, ADRA2C, MC5R, NFKBIE
PKCθ signaling in T lymphocytes	1.65	0.051	GRAP2, MAP3K7, MAP3K5, NFKBIE, MAP3K4, NFATC1
Hepatic cholestasis	1.50	0.043	MAP3K7, PRKCD, TGFB2, PRKCI, HNF4A, NFKBIE, MAP3K4
PI3K signaling in B lymphocytes	1.50	0.047	AKT3, PLCB4, PRKCI, NFKBIE, NFATC1, DAPP1
GnRH signaling	1.48	0.047	MAP3K7, PRKCD, MAP3K5, PLCB4, PRKCI, MAP3K4
Mismatch repair in eukaryotes	1.46	0.125	RPA1, MSH2
Erythropoietin signaling	1.45	0.060	PRKCD, AKT3, PRKCI, NFKBIE
Superpathway of Geranylgeranyldiphosphate biosynthesis I (via mevalonate)	1.41	0.118	ACAT2, GGPS1
NF-κB signaling	1.37	0.041	MAP3K7, AKT3, NTRK2, NFKBIE, TBK1, IGF2R, FGFR1
D-myo-inositol (1,4,5)-trisphosphate degradation	1.37	0.111	IMPA2, BPNT1
B cell receptor signaling	1.34	0.040	MAP3K7, AKT3, MAP3K5, NFKBIE, MAP3K4, NFATC1, DAPP1
NF-κB activation by viruses	1.33	0.055	PRKCD, AKT3, PRKCI, NFKBIE
STAT3 pathway	1.33	0.055	SOCS5, NTRK2, IGF2R, FGFR1
Role of NFAT in cardiac hypertrophy	1.31	0.039	MAP3K7, PRKCD, AKT3, PLCB4, SLC8A1, TGFB2, PRKCI
NGF signaling	1.31	0.047	MAP3K7, PRKCD, AKT3, MAP3K5, MAP3K4

\*IPA identified 42 pathways significantly enriched in the HYP black module. Only those pathways that also contain well-connected genes are shown. Ratio: Number of pathway genes in the black module divided by the total number of genes in the pathway.

of glycogen (see Raththagala *et al.* 2015) and is thus key to cellular energy supply and metabolism. Another hub gene in both modules, *NTPCR*, hydrolyzes nucleosides (e.g. GTP and ATP) and thus may also be important for energy homeostasis. *AARS2*, which is highly connected in the greenyellow module and appears in the black module as well, catalyzes the attachment of amino acid residues to tRNA (reviewed by Gillet & Felden 2001) and is thus critical for protein translation. Each of these genes is evolutionarily ancient, with homologues found in most taxa including plants and prokaryotes, reflecting their ubiquitous roles in basic cellular functioning. Their specific roles in behavior are unclear in the context of this study, other than that they support basic functions in brain regions that are

known to be active during territorial defense and other social behaviors.

To better understand the relationships among the genes in the two modules correlated with behavior, we conducted IPA, which reveals enrichment of gene pathways with known functions. Each of the top three pathways in the MeA greenyellow module involved nuclear receptor signaling (Table 1). The glucocorticoid receptor signaling pathway represents a particularly interesting finding because Horton and Holberton (2010) found that during the parental provisioning stage of the breeding season, TS males had lower levels of plasma corticosterone (CORT) than WS males. To test whether this hormonal difference may mediate known

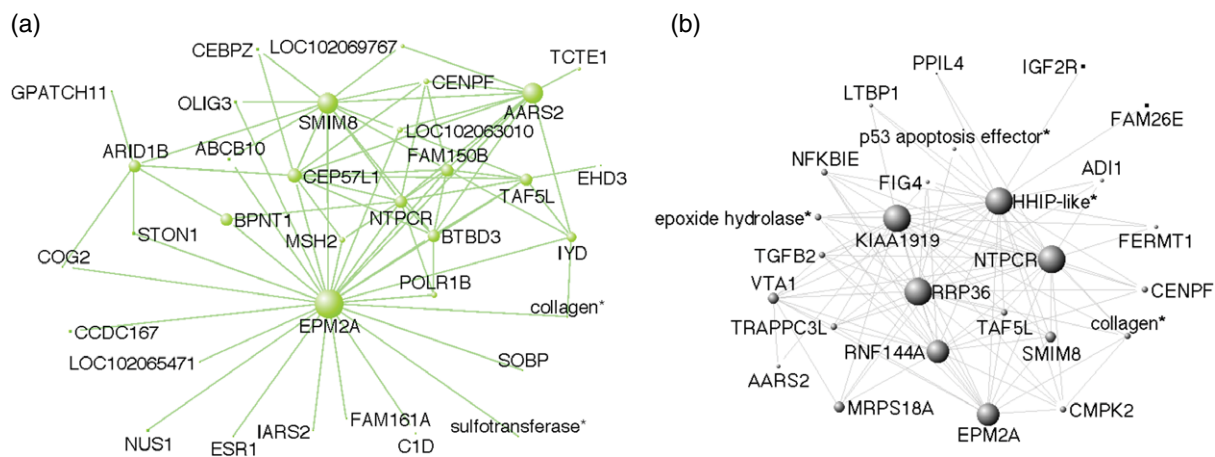


**Figure 4: Connectivity in the MeA greenyellow and HYP black networks.** Only the (a) 75 (MeA) or (b) 100 (HYP) strongest connections among the top 50 most well-connected genes (determined using kIN) are shown. Node size represents the degree of connectivity. \*Where available, gene description for LOC genes are used. See Tables S2 and S4 for LOC gene designations.

morph differences in parental provisioning rates, they experimentally raised plasma CORT in TS birds and blocked CORT in the WS birds. These manipulations essentially eliminated morph differences in parental provisioning rates (Horton & Holberton 2009). Although we did not collect tissue during the parental phase, our results confirm that genes in the CORT signaling pathway are differentially expressed in the morphs and may play a role in morph-dependent behaviors.

Perhaps our most compelling finding is that the MeA module that was correlated with both morph and singing was enriched for genes in the ER signaling pathway (Table 1). Expression of  $ER\alpha$ , which is encoded by the gene estrogen receptor 1 (*ESR1*), has been shown in previous studies to be correlated with territorial aggression and parenting behavior in this and other species. For example, in dark-eyed juncos (*Junco hyemalis*), aggressive responses to STI were positively correlated with expression of  $ER\alpha$  in the ventral telencephalon (containing the MeA) and negatively correlated in HYP (which in that study included POM and VMH) (Rosvall *et al.* 2012). In a previous study, we reported that in white-throated sparrows,  $ER\alpha$  mRNA is differentially expressed in MeA and several other brain regions (Horton *et al.* 2014a). In that study, expression of  $ER\alpha$  in both the MeA and PVN predicted song rate in response to STI, a correlation that persisted even when morph and plasma levels of testosterone and estradiol were held constant. Mediation analysis showed in fact that singing in response to STI was better predicted by  $ER\alpha$  expression in MeA than by morph (Horton *et al.* 2014a). In this study,  $ER\alpha$  in the MeA module was associated with both morph and singing, which replicates our previous findings and supports our hypothesis that this gene may play a key role in the behavioral polymorphism in this species and the evolution of alternative reproductive strategies generally (Cushing *et al.* 2008; Maney *et al.* 2015).

In addition to *ESR1*, other genes with known relationships with estrogen signaling were located in the modules

correlated with singing. For example, the expression of *TAF5L*, a transcription factor in the ER signaling pathway, was well connected in both the MeA greenyellow and HYP black modules (Fig. 4). Thompson *et al.* (2012) showed that *TAF5L* expression was highly correlated with the expression of immediate early genes such as *EGR1* and *FOS* in the song control nuclei of white-crowned sparrows (*Zonotrichia leucophrys*), a congener of the white-throated sparrow. Because Thompson *et al.* quantified expression in the motor nuclei that are most active during singing, their results suggest that *TAF5L* expression may be related to activity generally; it may also be altered by increasing local concentrations of estradiol (Fong *et al.* 2007), which is released in nearby regions in response to hearing conspecific song (Remage-Healey *et al.* 2008).

When bound with ligand, ERs act via two main mechanisms: genomic and nongenomic. In the canonical genomic pathway, the receptor binds estradiol inside the cytoplasm, translocates to the nucleus and acts as a transcription factor. If  $ER\alpha$  mediates morph differences in behavior via genomic mechanisms, we might expect it to regulate the transcription of a large number of other genes and to be well connected in the modules correlated with behavior. It does not, however, appear to act as a hub in either network (Fig. 4). It is possible that  $ER\alpha$  may regulate morph-dependent behaviors via nongenomic mechanisms such as membrane-bound receptors. For example,  $ER\alpha$  can act in a nongenomic fashion by interacting with the metabotropic glutamate receptor (mGluR1; Meitzen & Mermelstein 2011).  $ER\alpha$  can also induce phosphorylation of the membrane-associated protein Shc, which then interacts with two other proteins, Grb2 and Sos, to initiate intracellular events (Song *et al.* 2002). Genes for proteins critical to each of these nongenomic mechanisms, *GRM1* and *SOS1*, are both found in the MeA greenyellow module meaning that similar to *ESR1*, their expression depends on morph and is linked with behavior.

When estradiol acts via nongenomic mechanisms, resulting changes in intracellular activity, such as MAPK activation

and firing, are rapid and likely short-lived. Therefore, intracellular events downstream of ER $\alpha$  activation may not be detectable by measuring gene expression many hours after the last STI, nor would they necessarily be correlated with behavior. We intentionally delayed sampling until 24 h after the last STI because we were not interested in the effects of behavioral responses on gene expression, but rather the opposite – we wanted to discover genes related to the motivation to respond to challenge rather than engaging in the response itself. Other researchers have published lists of genes that are induced by STI in wild songbirds; for example, of all the genes induced by STI in the HYP of song sparrows (*Melospiza melodia*; Mukai *et al.* 2009), only two genes, *TBCE* and *PEX13*, were in a module associated with behavior in this study (HYP black module). According to Mukai *et al.*, many other genes are selectively expressed as a result of engaging in territorial defense; we would expect to find robust morph differences in the expression of those genes immediately following STI.

Synaptic plasticity has been associated with behavioral differences between sexes in zebrafish (Wong *et al.* 2014) and vocal learning in zebra finches (Hilliard *et al.* 2012). Enriched pathways and GO terms in both the MeA greenyellow and HYP black modules can be broadly associated with synapse function or activity. In the MeA, enriched GO terms were related to energy production and vesicle transport (e.g. mitochondria and microtubules). In the HYP black module, three of the six genes annotated with the GO term 'extracellular matrix organization' are hub genes (Table S5). Both modules were enriched for genes related to retinoic acid signaling. In the HYP black module, these terms were 'isoprenoid biosynthetic process', 'retinoic acid receptor (RAR) activation' and 'vitamin D receptor/ retinoid X receptor (VDR/RXR) activation'. The MeA greenyellow module was enriched for genes belonging to the peroxisome proliferator-activated receptor (PPAR) $\alpha$ /RXR $\alpha$  activation pathway. Both the extracellular matrix and retinoid signaling play important roles in synaptic function and plasticity (Frischknecht & Gundelfinger 2012; Shearer *et al.* 2012). These results suggest that morph differences in vocal aggression may relate to processes involved in synaptic plasticity.

Because we did not continuously monitor the birds' behavior during the hours immediately preceding tissue collection, we must consider the possibility that the morph differences in gene expression we found were related to territorial behavior that we did not observe. Previous studies on songbirds have shown that large numbers of genes are regulated by either experience (e.g. listening to song) or behavior (e.g. singing) (Drnevich *et al.* 2012; Mukai *et al.* 2009; Whitney *et al.* 2014). Formica *et al.* (2004) have shown that WS and TS birds prefer different types of habitat; WS males choose territories with more neighbors and therefore higher frequencies of agonistic encounters than TS males (see also Formica & Tuttle 2009). We believe that morph differences in habitat selection were unlikely to have played a key role in our findings here. First, although we cannot rule out effects of social niche partitioning, in this population, the morphs are fairly evenly distributed and tend to occupy the same types of habitat (Horton *et al.* 2014b). Second, to determine whether any of the modules were correlated with potential neuronal

responses to stimuli, we examined the expression of an immediate early gene, *EGR1*. *EGR1* expression, however, was not correlated with either of the modules associated with morph and song (Fig. 2). Note, however, that singing is not known to be correlated with Egr-1 protein induction in MeA (Earp & Maney 2012), so this measure may not indicate whether birds were engaging in territorial defense. Finally, we and others have shown significant morph differences in behavior in controlled conditions in the laboratory; WS males sang at higher rates and were more aggressive than TS birds (Maney & Goodson 2011; Maney *et al.* 2009; Swett 2007) even when social conditions were identical. These differences persisted despite similar levels of plasma sex steroids in the two morphs, supporting the hypothesis that morph differences in neural sensitivity to sex steroids, which could take the form of morph differences in receptor numbers or distribution, may underlie morph differences in territorial behavior.

The WGCNA identified many more modules in the HYP than the MeA network, even though both networks were constructed using the same parameters. One possible explanation for the larger number of modules in the HYP network is that it reflects the more heterogeneous nature of the HYP samples. Gene expression patterns are known to depend on brain region (Balakrishnan *et al.* 2014; Drnevich *et al.* 2012; Whitney *et al.* 2014). Our HYP punches contained several hypothalamic nuclei (see *Materials and methods* and Fig. S1) in which genes may be differentially regulated. In networks that are built using samples collected from multiple, distinct brain regions or nuclei, modules that distinguish these individual nuclei or specific brain regions can be identified (Drnevich *et al.* 2012; Konopka *et al.* 2012; Oldham *et al.* 2006). We were unable to perform this type of analysis with our dataset because our network was built using one sample type (HYP). Although we are unaware of genes that define only one sub-region of the HYP, we have previously shown that morph differences in ER $\alpha$  expression are dependent on brain region. We previously showed, for example, that ER $\alpha$  expression is higher in TS than WS birds in VMH and caudal POM, but higher in WS than TS birds in PVN (Horton *et al.* 2014a); both VMH and PVN were present in our HYP sample. Heterogeneity may thus explain why, although we replicated our previous finding of differential expression of ER $\alpha$  in MeA (Horton *et al.* 2014a), we could not detect differential expression of ER $\alpha$  in our HYP sample. In dark-eyed juncos, expression of ER $\alpha$  in HYP was negatively correlated with territorial aggression (Rosvall *et al.* 2012). Here, we were unable to detect a correlation between song rate and ER $\alpha$  in HYP and the ESR1 gene was not located within the HYP black module. In future studies, it may be important to conduct RNA-seq on smaller samples limited to a single region in order to detect morph differences in gene expression within regions with distinct functions and cell types.

Our results show the profound effects of the ZAL2/2<sup>m</sup> rearrangement on gene expression. Our two modules of interest, MeA greenyellow and HYP black, were composed primarily of genes captured by the inversion (see Figs. 2, 3). Standard network analysis groups genes into modules based on co-expression. The usual interpretation of these modules, which we have presented above, is that

co-expressed genes are functionally related. As a result, a significant fraction of genes within a module often represent similar GO categories or canonical pathways (Langfelder *et al.* 2011; Oldham *et al.* 2006). However, multiple mechanisms can influence gene–gene correlations, including higher order chromosome configuration and epigenetic regulation (Gaiteri *et al.* 2014). We must also consider a second interpretation; in our analysis, genes may be grouped into co-expression modules because of co-localization within the differentiating region. We did not observe enrichment of ZAL2/2<sup>m</sup> genes in any other modules, suggesting that the inversion was a facilitating factor in the emergence of the MeA greenyellow and HYP black modules. In support of this alternative explanation, we found that all of the chromosome 2 genes within the MeA greenyellow and HYP black modules were located within the inversion; in other words, none of the chromosome 2 genes within these modules were located in the recombining regions of chromosome 2, outside the inversion. We also found significant overlap in gene membership between the modules, and most (70/84) of these shared genes were located within the inversion. Therefore, the traditional interpretation that genes within a co-expression network are connected because they act in the same pathway or biological processes represents only one of the several possible mechanisms driving gene–gene correlations. It is also important to note that because of the large morph difference in singing in this study (Fig. 1a), it is difficult to dissociate that trait from plumage morph; the only modules correlated with singing were also correlated with morph. Placement of ESR1 within the MeA greenyellow module confirmed that our network analysis correctly identified a gene known to predict song rate independently of morph (Horton *et al.* 2014a). Whether song rate is reliably predicted by other genes in the module, however, is difficult to test in this dataset because of our relatively small sample size. Follow-up studies will be necessary to evaluate the potential roles of other promising genes in territorial aggression.

The white-throated sparrow is a useful model system in which to study the consequences of an inversion on gene expression. By suppressing recombination between alleles, chromosomal rearrangements can foster the evolution of co-adapted alleles or ‘supergenes’ (Dobzhansky 1970). Inversions that encompass multiple genes involving a suite of phenotypic traits might therefore maintain both behavioral and color polymorphism within a species (reviewed in McKinnon & Pierotti 2010). Alternatively, a single gene with pleiotropic effects might be responsible for both behavioral and color polymorphism. Likely candidates are transcription factors and hormones. Transcription factors have the capacity to coordinate the expression of multiple genes that share a *cis*-regulatory region. Hormones can activate transcription factors and act through nongenomic signaling pathways. We cannot determine from this study whether co-adapted alleles or a small number of pleiotropic genes can explain the behavioral polymorphism. It will be interesting to determine in future studies the extent to which manipulating expression of a single gene can influence behavior in this species.

## References

- Anders, S., Pyl, P.T. & Huber, W. (2015) HTSeq—a Python framework to work with high-throughput sequencing data. *Bioinformatics* **31**, 166–169.
- Anholt, R.R. & Mackay, T.F. (2012) Genetics of aggression. *Annu Rev Genet* **46**, 145–164.
- Balakrishnan, C.N., Mukai, M., Gonser, R.A., Wingfield, J.C., London, S.E., Tuttle, E.M. & Clayton, D.F. (2014) Brain transcriptome sequencing and assembly of three songbird model systems for the study of social behavior. *PeerJ* **2**, e396.
- Collins, C.E. & Houtman, A.M. (1999) Tan and white color morphs of white-throated sparrows differ in their non-song vocal responses to territorial intrusion. *Condor* **101**, 842–845.
- Cushing, B.S., Perry, A., Musatov, S., Ogawa, S. & Papademetriou, E. (2008) Estrogen receptors in the medial amygdala inhibit the expression of male prosocial behavior. *J Neurosci* **28**, 10399–10403.
- Davis, J.K., Mittel, L.B., Lowman, J.J., Thomas, P.J., Maney, D.L., Martin, C.L. & Thomas, J.W. (2011) Haplotype-based genomic sequencing of a chromosomal polymorphism in the white-throated sparrow (*Zonotrichia albicollis*). *J Hered* **102**, 380–390.
- Dobin, A., Davis, C.A., Schlesinger, F., Drenkow, J., Zaleski, C., Jha, S., Batut, P., Chaisson, M. & Gingeras, T.R. (2013) STAR: ultrafast universal RNA-seq aligner. *Bioinformatics* **29**, 15–21.
- Dobzhansky, T. (1970) *Genetics of the Evolutionary Process*. Columbia University Press, New York, NY.
- Drnevich, J., Replogle, K.L., Lovell, P., Hahn, T.P., Johnson, F., Mast, T.G., Nordeen, E., Nordeen, K., Strand, C., London, S.E., Mukai, M., Wingfield, J.C., Arnold, A.P., Ball, G.F., Brenowitz, E.A., Wade, J., Mello, C.V. & Clayton, D.F. (2012) Impact of experience-dependent and -independent factors on gene expression in songbird brain. *Proc Natl Acad Sci* **109**, 17245–17252.
- Earp, S.E. & Maney, D.L. (2012) Birdsong: is it music to their ears? *Front Evol Neurosci* **4**, 14.
- Falls, J.B. (1988) Does song deter territorial intrusion in white-throated sparrows (*Zonotrichia albicollis*). *Can J Zool* **66**, 206–211.
- Falls, J.B. & Kopachena, J.G. (2010) White-throated sparrow (*Zonotrichia albicollis*). In Poole A. (ed), *The Birds of North America Online*. Cornell Lab of Ornithology, Ithaca, NY.
- Filteau, M., Pavey, S.A., St-Cyr, J. & Bernatchez, L. (2013) Gene coexpression networks reveal key drivers of phenotypic divergence in lake whitefish. *Mol Biol Evol* **30**, 1384–1396.
- Flicek, P., Amode, M.R., Barrell, D. *et al.* (2014) Ensembl 2014. *Nucleic Acids Res* **42**, D749–D755.
- Fong, C.J., Burgoon, L.D., Williams, K.J., Forgacs, A.L. & Zacharewski, T.R. (2007) Comparative temporal and dose-dependent morphological and transcriptional uterine effects elicited by tamoxifen and ethynylestradiol in immature, ovariectomized mice. *BMC Genomics* **8**, 151.
- Formica, V.A. & Tuttle, E.M. (2009) Examining the social landscapes of alternative reproductive strategies. *J Evol Biol* **22**, 2395–2408.
- Formica, V.A., Gonser, R.A., Ramsay, S. & Tuttle, E.M. (2004) Spatial dynamics of alternative reproductive strategies: the role of neighbors. *Ecology* **85**, 1125–1136.
- Frischknecht, R. & Gundelfinger, E.D. (2012) The brain's extracellular matrix and its role in synaptic plasticity. *Adv Exp Med Biol* **970**, 153–171.
- Fuller, T.F., Ghazalpour, A., Aten, J.E., Drake, T.A., Lusis, A.J. & Horvath, S. (2007) Weighted gene coexpression network analysis strategies applied to mouse weight. *Mamm Genome* **18**, 463–472.
- Gaiteri, C., Ding, Y., French, B., Tseng, G.C. & Sibille, E. (2014) Beyond modules and hubs: the potential of gene coexpression networks for investigating molecular mechanisms of complex brain disorders. *Genes Brain Behav* **13**, 13–24.
- Ghazalpour, A., Doss, S., Zhang, B., Wang, S., Plaisier, C., Castellanos, R., Brozell, A., Schadt, E.E., Drake, T.A., Lusis, A.J. & Horvath, S. (2006) Integrating genetic and network analysis to characterize genes related to mouse weight. *PLoS Genet* **2**, e130.



- Gillet, R. & Felden, B. (2001) Emerging views on tmRNA-mediated protein tagging and ribosome rescue. *Mol Microbiol* **42**, 879–885.
- Goodson, J.L. (2005) The vertebrate social behavior network: evolutionally themes and variations. *Horm Behav* **48**, 11–22.
- Goodson, J.L., Evans, A.K. & Soma, K.K. (2005) Neural responses to aggressive challenge correlate with behavior in non-breeding sparrows. *Neuroreport* **16**, 1719–1723.
- Hilliard, A.T., Miller, J.E., Fraley, E.R., Horvath, S. & White, S.A. (2012) Molecular microcircuitry underlies functional specification in a basal ganglia circuit dedicated to vocal learning. *Neuron* **73**, 537–552.
- Horton, B.M. & Holberton, R.L. (2009) Corticosterone manipulations alter morph-specific nestling provisioning behavior in male white-throated sparrows, *Zonotrichia albicollis*. *Horm Behav* **56**, 510–518.
- Horton, B.M. & Holberton, R.L. (2010) Morph-specific variation in baseline corticosterone and the adrenocortical response in breeding white-throated sparrows (*Zonotrichia albicollis*). *Auk* **127**, 9.
- Horton, B.M., Hauber, M.E. & Maney, D.L. (2012) Morph matters: aggression bias in a polymorphic sparrow. *PLoS One* **7**, e48705.
- Horton, B.M., Hu, Y., Martin, C.L., Bunke, B.P., Matthews, B.S., Moore, I.T., Thomas, J.W. & Maney, D.L. (2013) Behavioral characterization of a white-throated sparrow homozygous for the ZAL2(m) chromosomal rearrangement. *Behav Genet* **43**, 60–70.
- Horton, B.M., Hudson, W.H., Ortlund, E.A., Shirk, S., Thomas, J.W., Young, E.R., Zinzow-Kramer, W.M. & Maney, D.L. (2014a) Estrogen receptor alpha polymorphism in a species with alternative behavioral phenotypes. *Proc Natl Acad Sci U S A* **111**, 1443–1448.
- Horton, B.M., Moore, I.T. & Maney, D.L. (2014b) New insights into the hormonal and behavioural correlates of polymorphism in white-throated sparrows. *Anim Behav* **93**, 207–219.
- Hu, Z., Mellor, J., Wu, J. & DeLisi, C. (2004) VisANT: an online visualization and analysis tool for biological interaction data. *BMC Bioinformatics* **5**, 17.
- Huang da, W., Sherman, B.T. & Lempicki, R.A. (2009) Systematic and integrative analysis of large gene lists using DAVID bioinformatics resources. *Nat Protoc* **4**, 44–57.
- Huynh, L.Y., Maney, D.L. & Thomas, J.W. (2011) Chromosome-wide linkage disequilibrium caused by an inversion polymorphism in the white-throated sparrow (*Zonotrichia albicollis*). *Heredity (Edinb)* **106**, 537–546.
- Kidd, J.M., Cooper, G.M., Donahue, W.F. *et al.* (2008) Mapping and sequencing of structural variation from eight human genomes. *Nature* **453**, 56–64.
- Knapton, R.W. & Falls, J.B. (1983) Differences in parental contribution among pair types in the polymorphic white-throated Sparrow. *Can J Zool* **61**, 1288–1292.
- Konopka, G., Friedrich, T., Davis-Turak, J., Winden, K., Oldham, M.C., Gao, F., Chen, L., Wang, G.Z., Luo, R., Preuss, T.M. & Geschwind, D.H. (2012) Human-specific transcriptional networks in the brain. *Neuron* **75**, 601–617.
- Kopachena, J.G. & Falls, J.B. (1993a) Aggressive performance as a behavioral correlate of plumage polymorphism in the white-throated sparrow (*Zonotrichia albicollis*). *Behaviour* **124**, 249–266.
- Kopachena, J.G. & Falls, J.B. (1993b) Reevaluation of morph-specific variations in parental behavior of the white-throated sparrow. *Wilson Bull* **105**, 48–59.
- Langfelder, P. & Horvath, S. (2008) WGCNA: an R package for weighted correlation network analysis. *BMC Bioinformatics* **9**, 559.
- Langfelder, P., Zhang, B. & Horvath, S. (2008) Defining clusters from a hierarchical cluster tree: the Dynamic Tree Cut package for R. *Bioinformatics* **24**, 719–720.
- Langfelder, P., Luo, R., Oldham, M.C. & Horvath, S. (2011) Is my network module preserved and reproducible? *PLoS Comput Biol* **7**, e1001057.
- Li, H., Handsaker, B., Wysoker, A., Fennell, T., Ruan, J., Homer, N., Marth, G., Abecasis, G. & Durbin, R. (2009) The sequence alignment/map format and SAMtools. *Bioinformatics* **25**, 2078–2079.
- Love, M.I., Huber, W. & Anders, S. (2014) Moderated estimation of fold change and dispersion for RNA-seq data with DESeq2. *Genome Biol* **15**, 550.
- Lowther, J.K. (1961) Polymorphism in the white-throated sparrow, *Zonotrichia albicollis* (Gmelin). *Can J Zool* **39**, 281–292.
- Lowther, J. (1962) *Colour and behavioral polymorphism in the white-throated sparrow, Zonotrichia albicollis*. PhD thesis. University of Toronto, Toronto, Ontario, Canada.
- Ma, J. & Amos, C.I. (2012) Investigation of inversion polymorphisms in the human genome using principal components analysis. *PLoS One* **7**, e40224.
- Maney, D.L. (2008) Endocrine and genomic architecture of life history trade-offs in an avian model of social behavior. *Gen Comp Endocrinol* **157**, 275–282.
- Maney, D.L. & Goodson, J.L. (2011) Neurogenomic mechanisms of aggression in songbirds. *Adv Genet* **75**, 83–119.
- Maney, D.L., Goode, C.T., Lange, H.S., Sanford, S.E. & Solomon, B.L. (2008) Estradiol modulates neural responses to song in a seasonal songbird. *J Comp Neurol* **511**, 173–186.
- Maney, D.L., Lange, H.S., Raees, M.Q., Reid, A.E. & Sanford, S.E. (2009) Behavioral phenotypes persist after gonadal steroid manipulation in white-throated sparrows. *Horm Behav* **55**, 113–120.
- Maney, D.L., Horton, B.M. & Zinzow-Kramer, W.M. (2015) Estrogen receptor alpha as a mediator of life-history trade-offs. *Integr Comp Biol* **55**, 323–331.
- McKenna, A., Hanna, M., Banks, E., Sivachenko, A., Cibulskis, K., Kernysky, A., Garimella, K., Altshuler, D., Gabriel, S., Daly, M. & DePristo, M.A. (2010) The genome analysis toolkit: a MapReduce framework for analyzing next-generation DNA sequencing data. *Genome Res* **20**, 1297–1303.
- McKinnon, J.S. & Pierotti, M.E. (2010) Colour polymorphism and correlated characters: genetic mechanisms and evolution. *Mol Ecol* **19**, 5101–5125.
- Meitzen, J. & Mermelstein, P.G. (2011) Estrogen receptors stimulate brain region specific metabotropic glutamate receptors to rapidly initiate signal transduction pathways. *J Chem Neuroanat* **42**, 236–241.
- Mukai, M., Replogle, K., Drnevich, J., Wang, G., Wacker, D., Band, M., Clayton, D.F. & Wingfield, J.C. (2009) Seasonal differences of gene expression profiles in song sparrow (*Melospiza melodia*) hypothalamus in relation to territorial aggression. *PLoS One* **4**, e8182.
- Nelson, R.J. & Chiavegatto, S. (2001) Molecular basis of aggression. *Trends Neurosci* **24**, 713–719.
- O'Connell, L.A. & Hofmann, H.A. (2011) The vertebrate mesolimbic reward system and social behavior network: a comparative synthesis. *J Comp Neurol* **519**, 3599–3639.
- Oldham, M.C., Horvath, S. & Geschwind, D.H. (2006) Conservation and evolution of gene coexpression networks in human and chimpanzee brains. *Proc Natl Acad Sci U S A* **103**, 17973–17978.
- Raththagala, M., Brewer, M.K., Parker, M.W. *et al.* (2015) Structural mechanism of laforin function in glycogen dephosphorylation and lafora disease. *Mol Cell* **57**, 261–272.
- Remage-Healey, L., Maidment, N.T. & Schlinger, B.A. (2008) Forebrain steroid levels fluctuate rapidly during social interactions. *Nat Neurosci* **11**, 1327–1334.
- Romanov, M.N., Dodgson, J.B., Gonser, R.A., Tuttle, E.M. (2011) Comparative BAC-based mapping in the white-throated sparrow, a novel behavioral genomics model, using interspecies overgo hybridization. *BMC Research Notes* **4**, 211.
- Rosvall, K.A., Bergeon Burns, C.M., Barske, J., Goodson, J.L., Schlinger, B.A., Sengelaub, D.R. & Ketterson, E.D. (2012) Neural sensitivity to sex steroids predicts individual differences in aggression: implications for behavioural evolution. *Proc Biol Sci* **279**, 3547–3555.
- Shearer, K.D., Stoney, P.N., Morgan, P.J. & McCaffery, P.J. (2012) A vitamin for the brain. *Trends Neurosci* **35**, 733–741.
- Song, R.X., McPherson, R.A., Adam, L., Bao, Y., Shupnik, M., Kumar, R. & Santen, R.J. (2002) Linkage of rapid estrogen action to MAPK activation by ERalpha-Shc. *Mol Endocrinol* **16**, 116–127.

- Swett, M.B. (2007) *Hormonal mediation of a unique behavioral polymorphism in the white-throated sparrow (Zonotrichia albicollis)*. PhD thesis. University of Montana, Missoula, MT.
- Thomas, J.W., Caceres, M., Lowman, J.J., Morehouse, C.B., Short, M.E., Baldwin, E.L., Maney, D.L. & Martin, C.L. (2008) The chromosomal polymorphism linked to variation in social behavior in the white-throated sparrow (*Zonotrichia albicollis*) is a complex rearrangement and suppressor of recombination. *Genetics* **179**, 1455–1468.
- Thompson, C.K., Meitzen, J., Replogle, K., Drnevich, J., Lent, K.L., Wissman, A.M., Farin, F.M., Bammler, T.K., Beyer, R.P., Clayton, D.F., Perkel, D.J. & Brenowitz, E.A. (2012) Seasonal changes in patterns of gene expression in avian song control brain regions. *PLoS One* **7**, e35119.
- Thorncroft, H.B. (1975) A cytogenetic study of the white-throated sparrow, *Zonotrichia albicollis* (Gmelin). *Evolution* **29**, 611–621.
- Trivers, R.L. (1972) Parental investment and sexual selection. In Campbell, B. (ed), *Sexual Selection and the Descent of Man*. Aldine, Chicago, IL, pp. 136–179.
- Tuttle, E.M. (2003) Alternative reproductive strategies in the white-throated sparrow: behavioral and genetic evidence. *Behav Ecol* **14**, 425–432.
- Tuttle, E.M., Bergland, A.O., Korody, M.L., Brewer, M.S., Newhouse, D.J., Minx, P., Stager, M., Betuel, A., Cheviron, Z.A., Warren, W.C., Rusty, A., Gonser, R.A., & Balakrishnan, C.N. In review. The complete genome of the polymorphic white-throated sparrow.
- Watt, D.J. (1986) Plumage brightness index for white-throated sparrows. *J Field Ornithol* **57**, 105–113.
- White, M.J.D. (1977) *Animal Cytology and Evolution*. Cambridge University Press Archive, London.
- Whitney, O., Pfenning, A.R., Howard, J.T., Blatti, C.A., Liu, F., Ward, J.M., Wang, R., Audet, J.N., Kellis, M., Mukherjee, S., Sinha, S., Hartemink, A.J., West, A.E. & Jarvis, E.D. (2014) Core and region-enriched networks of behaviorally regulated genes and the singing genome. *Science* **346**, 1256780.
- Wingfield, J.C. & Hahn, T.P. (1994) Testosterone and territorial behavior in sedentary and migratory sparrows. *Anim Behav* **47**, 77–89.
- Wong, R.Y., McLeod, M.M. & Godwin, J. (2014) Limited sex-biased neural gene expression patterns across strains in zebrafish (*Danio rerio*). *BMC Genomics* **15**, 905.
- Wu, X. & Watson, M. (2009) CORNA: testing gene lists for regulation by microRNAs. *Bioinformatics* **25**, 832–833.
- Zhang, B. & Horvath, S. (2005) A general framework for weighted gene co-expression network analysis. *Stat Appl Genet Mol Biol* **4**, Article17.

## Acknowledgments

Sequencing of the superwhite genome and SNP calling between the reference assembly and the superwhite assembly were performed by the Roy J. Carver Biotechnology Center of the University of Illinois. RNA-seq for the HYP and MeA samples was conducted at the Yerkes Nonhuman Primate Genomics Core Laboratory. This work was supported by NSF grant SMA-1306132 to W.M.Z.-K. and D.L.M. and NIH grants R01MH082833 to D.L.M. and 1R21NIH102677 to D.L.M. and S.V.Y. The National Human Genome Research Institute Intramural Research program at the NIH supported J.W.T. The authors have no conflicts of interest to report.

## Supporting Information

Additional supporting information may be found in the online version of this article at the publisher's web-site:

**Figure S1:** Diagram of the locations of punches for (a) MeA and (b) HYP samples. Circles indicate punched regions. (a)

The MeA punch contained the ventromedial telencephalon, which is largely composed of the MeA. (b) The dorsal HYP punches contained the anterior hypothalamus (AH), the caudal portion of the POM and the PVN. The ventral punches included the VMH. AC, anterior commissure.

**Figure S2:** Overlap of genes between MeA and HYP modules. Modules in the MeA and HYP are presented in columns and rows, respectively. The number of genes shared by each MeA and HYP module is given in the table. The table is color-coded according to the  $-\log$  of the Fisher's exact test  $P$ -values, as indicated by the color bar on the right.

**Table S1:** Correlations between traits and MEs in the MeA. Numbers in each cell represent the correlation coefficient and  $P$ -values are in parentheses. The correlation coefficient values are depicted in the heatmap in Fig. 2a.

**Table S2:** MeA network data. This table contains chromosome location, corresponding zebra finch and chicken annotations, GS calculations, and intramodule connectivity for all genes analyzed in the WGCNA. Each row contains information on a gene annotated in the sparrow genome and present in the RNA-seq data. Columns (a) gene name, (b) gene description: LOC gene descriptions used in Fig. 4, (c) Ensembl-Gal: chicken Ensembl gene name, (d) Ensembl-Tg: zebra finch Ensembl gene name, (e) Chr-Gal: chromosome location in chicken, (f) ZAL2: whether or not the gene is located on chromosome 2 (see *Materials and methods* section for details), (g) inversion: for ZAL2 genes, whether or not the gene is located inside (i) or outside (o) the inversion, (h) module color: color of the module the gene was assigned to. Columns (i–p) contain the values for the correlation (GS) between gene expression and the indicated trait or gene (songs, morph, PC1 and *EGR1* expression), and the corresponding  $P$ -values (p.GS). (q) kIN: intramodule connectivity, calculated only for genes in the greenyellow module.

**Table S3:** Correlations between traits and MEs in the HYP. Numbers in each cell represent the correlation coefficient and  $P$ -values are in parentheses. The correlation coefficient values are depicted in the heatmap in Fig. 2b.

**Table S4:** HYP network data. Columns (a–p) are the same as in Table S2, (q) contains kIN for genes in the black module.

**Table S5:** GO terms significantly enriched in the modules correlated with song rate and morph. Each row represents an enriched term ( $P < 0.05$ ). Columns represent (a) module: module in which the term was enriched, (b) GO ID, (c) total number of genes annotated with that term, (d) expected number of genes in the module, (e) actual number of genes in the module, (f) enrichment  $P$ -value, (g) false discovery rate, (h) genes annotated by the term and present in the module, (i) GO term description, (j) GO term process. Terms with fewer than three members or with fewer than two members in the module of interest were removed from the list. \*Hub genes.

**File S1:** SNP calls between the reference genome and the superwhite genome used to generate the alternate ZAL2m contigs.

**File S2:** rRNA sequences added to the enhanced reference genome.

**File S3:** Mitochondrial sequences added to the enhanced reference genome.

Copyright of Genes, Brain & Behavior is the property of Wiley-Blackwell and its content may not be copied or emailed to multiple sites or posted to a listserv without the copyright holder's express written permission. However, users may print, download, or email articles for individual use.